Available online at www.sciencedirect.com
SCIENCE DIRECT®
Journal of Colloid and Interface Science 265 (2003) 83–92
JOURNAL OF Colloid and Interface Science
www.elsevier.com/locate/jcis

Miscibility behavior of dipalmitoylphosphatidylcholine with a single-chain partially fluorinated amphiphile in Langmuir monolayers

Takato Hiranita,[a] Shohei Nakamura,[a] Masaki Kawachi,[a] Hélène M. Courrier,[b,c] Thierry F. Vandamme,[c] Marie Pierre Krafft,[b,*] and Osamu Shibata [a,*,1]

[a] *Department of Molecular Bioformatics, Graduate School of Pharmaceutical Sciences, Kyushu University, 3-1-1 Maidashi, Higashi-ku, Fukuoka 812-8582, Japan*

[b] *Centre National de la Recherche Scientifique, Institut Charles Sadron (UPR 22), 6, rue Boussingault, 67083 Strasbourg Cedex, France*

[c] *Laboratoire de Chimie Thérapeutique et Nutritionnelle, Biodisponibilité Tissulaire et Cellulaire, Faculté de Pharmacie, Université Louis Pasteur, 67401 Illkirch Cedex, France*

Received 12 November 2002; accepted 1 May 2003

Abstract

Surface pressure–area, surface potential–area, and dipole moment–area isotherms were obtained for monolayers made from a partially fluorinated surfactant, (perfluorooctyl)undecyldimorpholinophosphate (F8H11DMP), dipalmitoylphosphatidylcholine (DPPC), and their combinations. Monolayers, spread on a 0.15 M NaCl subphase, were investigated at the air/water interface by the Wilhelmy method, ionizing electrode method, and fluorescence microscopy. Surface potentials were analyzed using the three-layer model proposed by Demchak and Fort. The contribution of the dimorpholinophosphate polar head group of F8H11DMP to the vertical component of the dipole moment was estimated to be 4.99 D. The linear variation of the phase transition pressure as a function of F8H11DMP molar fraction (X_{F8H11DMP}) demonstrated that DPPC and F8H11DMP are miscible in the monolayer. This result was confirmed by deviations from the additivity rule observed when plotting the molecular areas and the surface potentials as a function of X_{F8H11DMP} over the whole range of surface pressures investigated. Assuming a regular surface mixture, the Joos equation, which was used for the analysis of the collapse pressure of mixed monolayers, allowed calculation of the interaction parameter ($\xi = -1.3$) and the energy of interaction ($\Delta\varepsilon = 537\ \mathrm{J\,mol^{-1}}$) between DPPC and F8H11DMP. The miscibility of DPPC and F8H11DMP within the monolayer was also supported by fluorescence microscopy. Examination of the observed flower-like patterns showed that F8H11DMP favors dissolution of the ordered LC phase domains of DPPC, a feature that may be key to the use of phospholipid preparations as lung surfactants.

Keywords: Langmuir monolayers; Fluorinated surfactants; Surface potentials; Surface dipole moments; Two-dimensional phase diagrams; π–A isotherm; ΔV–A isotherm; Fluorescence microscopy

1. Introduction

Fluorocarbons (FCs) are thermally, chemically, and biologically inert and display high gas-dissolving capacities, low surface tension, high fluidity, excellent spreading characteristics, and low solubility in water [1]. As a unique feature, they are highly *hydro*phobic and *lipo*phobic at the same time. These unique properties have triggered research on a range of biomedical applications. Perfluorooctyl bromide ($C_8F_{17}Br$, PFOB) is being investigated for use in the form of a FC-in-water emulsion for delivering oxygen to tissues at risk of hypoxia [2,3]. FC-containing injectable micrometer-size gas bubbles are commercially available for use as contrast agents for ultrasound diagnostic imaging [4]. In its neat form, PFOB is being investigated for the delivery of drugs and genetic material to the lung [3]. FCs and fluorinated amphiphiles also allow the formation of multiphase compartmented systems that have potential as microreservoirs, microreactors, and templates [1,5].

We have reported that partially fluorinated amphiphiles derived from the dimorpholinophosphate polar head group,

* Corresponding authors.
E-mail addresses: krafft@ics.u-strasbg.fr (M.P. Krafft), shibata@phar.kyushu-u.ac.jp (O. Shibata).
[1] Mailing address: Department of Molecular Bioformatics, Graduate School of Pharmaceutical Sciences, Kyushu University, 3-1-1 Maidashi, Higashi-ku, Fukuoka 812-8582, Japan.

0021-9797/$ – see front matter
doi:10.1016/S0021-9797(03)00483-1

$C_nF_{2n+1}(CH_2)_mOP(O)[N(CH_2CH_2)_2O]_2$ (FnHmDMPs), allow the preparation of water-in-PFOB reverse emulsions and microemulsions with potential for controlled-release pulmonary delivery of drugs [6,7]. These emulsions were shown to deliver homogeneous and reproducible doses of a tracer using metered-dose inhalers pressurized with hydrofluoroalkanes [8]. A water-in-PFOB emulsion stabilized with F8H11DMP, which had been selected as the most effective emulsifier, was harmless toward human lung cultured cells [9]. In another type of application, a water-in-FC microemulsion based on F8H11DMP was used to investigate the perturbation of water dynamics as a function of confining size [10].

In a recent study, we found that depositing a water-in-PFOB microemulsion (formulated with F8H11DMP) on a dipalmitoylphosphatidylcholine (DPPC) monolayer, used as a lung surfactant model, led to the adsorption of F8H11DMP at the FC/water interface and to the formation of a mixed DPPC/F8H11DMP monolayer [11]. The results suggested that fluorocarbon microemulsions (or the fluorinated surfactant they contain) may facilitate the spreading of DPPC (which is the main component of lung surfactant) by preventing the formation of liquid condensed (LC) DPPC domains. Mixed monolayers made from combinations of hydrogenated and fluorinated surfactants have been reported [12,13]. The monolayer behavior of mixtures of carboxylic acids or alcohols with DPPC or related phosphatidylcholines has also been investigated [14]. One of us reported that DPPC and perfluorinated carboxylic acids formed partially miscible monolayers [15,16]. The interaction between the two amphiphiles was strong, suggesting that the attractive force between the two polar head groups contributes more strongly to miscibility than the hydrophobic interactions that exist between the long alkyl chains [15]. Partially fluorinated carboxylic acids were also shown to form miscible monolayers with DPPC [17].

We present here a study of the Langmuir monolayer behavior of DPPC, F8H11DMP, and their mixtures at the air/water interface. Surface pressure (π)–, surface potential (ΔV)–, and dipole moment ($\mu_\perp$)–area (A) isotherms were obtained for the pure compounds and their mixtures. The surface potentials were analyzed using the three-layer model proposed by Demchak and Fort [18]. The phase behavior of the mixed monolayers was examined in terms of additivity of molecular surface areas or of surface potentials. The molecular interaction between monolayer components was investigated using the Joos equation. Finally, the monolayers were examined by fluorescence microscopy.

2. Experimental

The (perfluorooctyl)undecyldimorpholinophosphate F8H11DMP was synthesized as reported previously [19]. It was thoroughly purified by repeated recrystallizations from hexane. Its purity was controlled by ^{1}H, ^{31}P, and ^{13}C NMR (Bruker AC 200), and elemental analysis. DPPC was purchased from Avanti Polar Lipids; TLC showed one single spot. n-Hexane and ethanol came from Merck (Uvasol) and Nacalai Tesque, respectively. Sodium chloride (Nacalai Tesque) was heated at 1023 K for 24 h to remove any surface-active organic impurity.

2.1. Surface pressure–area isotherms

The surface pressure, π, was measured using an automated home-made Wilhelmy film balance. The surface pressure balance (Mettler Toledo, AG245) had a resolution of 0.01 mN m^{-1}. The pressure-measuring system was equipped with a filter paper (Whatman 541, periphery 4 cm). The trough was made from a 720 cm^2 Teflon-coated brass. The π–A isotherms were recorded at 298.2 K. The monolayer was compressed at a speed of 0.073 nm^2 molecule^{-1} min^{-1}; however, no influence of the compression rate (0.073 vs 0.2 nm^2 molecule^{-1} min^{-1}) was detected within the limits of the experimental error. The standard deviations for area and surface pressure measurements were $\sim$0.01 nm^2 and $\sim$0.1 mN m^{-1}, respectively. In all cases, the substrate solution was a 0.15 M NaCl solution prepared with thrice distilled water (surface tension, 72.7 mN m^{-1} at 293.2 K; resistivity, 18 MΩ cm).

2.2. Monolayers at the air–water interface

Solutions of DPPC or F8H11DMP (1 mM) were prepared in n-hexane/ethanol (9/1 v/v). Fifty microliters of the DPPC or F8H11DMP solutions was spread on the subphase. For each DPPC/F8H11DMP molar ratio, DPPC and F8H11DMP were first cosolubilized in n-hexane/ethanol (9/1 v/v), and 50 µl of the solution was spread on the subphase. The spreading solvent was allowed to evaporate for 15 min prior to compression.

2.3. Surface potential measurements

Surface potential was recorded upon compression of the monolayer spread on 0.15 M NaCl at 298.2 K. It was monitored using an ionizing ^{241}Am electrode placed 1–2 mm above the interface, while a reference electrode was dipped into the subphase. The standard deviations for area and surface potential measurements were $\sim$0.01 nm^2 and $\sim$5 mV, respectively. The other experimental conditions were the same as described in previous papers [20–23].

2.4. Fluorescence microscopy

Fluorescence was observed using an automated home-made Langmuir film balance (Cahn RG Langmuir float type; resolution 0.01 mN m^{-1}) equipped with a BM-1000 fluorescence microscope (U.S.I. System) [20]. The trough (effective area: 750 cm^2) was made from Teflon-coated brass.

Compression speed was 0.07 nm^2 $molecule^{-1}$ min^{-1}. Surface pressure and fluorescence microscopy images were recorded simultaneously upon compression. The fluorescent probe (1 mol%) was 3,6-bis(diethylamino)-9-(2-octadecylcarbonyl)phenyl chloride (R18, Molecular Probes). A 300 W xenon lamp (XL 300, Pneum) was used for fluorescence excitation. Excitation and emission wavelengths were selected by an appropriate beam splitter/filter combination (Mitutoyo band path filter 546 nm, cut filter Olympus 590 nm). The monolayer was observed using a 20-fold magnification, long-distance objective lens (Mitutoyo $f = 200$/focal length 20 mm). Micrographs were recorded with a video camera (757 JAI ICCD camera, Denmark) connected to the microscope, directly into computer memory via an online image processor (Vaio PCV-R53 Sony: Video Capture Soft). The entire optical setup was placed on an active vibration isolation unit (Model-AY-1812, Visolator, Japan). All measurements were performed at 298.2 K.

3. Results and discussion

3.1. Surface pressure–, surface potential–, and dipole moment–area isotherms

The π–A isotherms of monolayers made from pure DPPC or F8H11DMP spread on 0.15 M NaCl at 298.2 K are shown in Fig. 1a. The F8H11DMP isotherm, typical of a liquid expanded monolayer, was stable up to 46 mN m^{-1}. The collapsed area was 0.47 nm^2. The extrapolated area (0.86 nm^2) reflected the bulkiness of the dimorpholinophosphate (DMP) polar head group, which is larger than the cross section of a partially fluorinated chain (0.31 nm^2) [24]. The DPPC isotherm presented the characteristic first-order transition from the disordered liquid expanded (LE) phase to the ordered liquid condensed (LC) phase [25,26]. The phase transition surface pressure, π^{eq}, at a given temperature, is a characteristic quantity for a given lipid in a monolayer on a given subphase. For DPPC on pure water, $\pi^{eq} \sim 4$ mN m^{-1} at 293.2 K and shifts by $\partial\pi^{eq}/\partial T \sim +1.5$ mN m^{-1} K^{-1}, until a tricritical point is reached at $T_t \sim 316.2$ K [25]. On 0.15 M NaCl, π^{eq} of DPPC was ∼11.5 mN m^{-1} (0.66 nm^2) at 298.2 K, which shows that, allowing for the difference in temperature, 7.5 mN m^{-1}, the ionic strength does not have a strong effect on π^{eq}. Collapse of the DPPC monolayer occurred at 55 mN m^{-1} (0.39 nm^2); the extrapolated area was 0.52 nm^2.

The vertical component of the surface dipole moment, $\mu_\perp$, was calculated from the Helmholtz equation using the measured ΔV values,

$$\Delta V = \mu_\perp/\varepsilon_0\varepsilon A, \tag{1}$$

where ε_0 is the permittivity of vacuum and ε the mean permittivity of the monolayer (which is assumed to be 1).

The variations of ΔV and $\mu_\perp$ as a function of A for DPPC and F8H11DMP monolayers are shown in Figs. 1b and 1c. Upon compression, the F8H11DMP monolayer goes through three successive phases. For areas larger than ∼3 nm^2 (phase 1) ΔV is null. The F8H11DMP molecules lie flat on the subphase's surface, all the molecule's subunits, i.e., the DMP group, the hydrocarbon spacer, and the fluorocarbon tail chain (which are both hydrophobic) being in contact with the subphase. The monolayer likely consists of a gas phase.

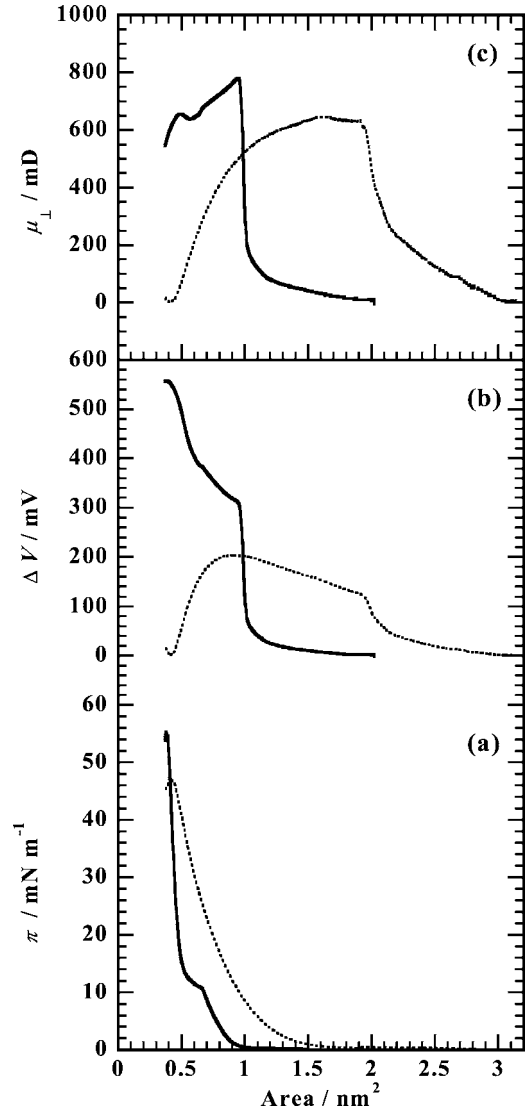

Fig. 1. (a) Surface pressure (π)-area (A) isotherms, (b) surface potential (ΔV)–A isotherms, and (c) surface dipole moment ($\mu_\perp$)–A isotherms of DPPC (solid line) and F8H11DMP (dotted line) monolayers on 0.15 M NaCl at 298.2 K.

Upon compression, the hydrophobic moieties come closer together and the molecules progressively stand up at an angle with the surface (phase 2). It is noteworthy that the onset of the ΔV increase occurs at a larger area than the π^{eq} onset, suggesting that ΔV is a more sensitive detector of surface activity than π. ΔV reaches ∼120 mV at 2 nm^2 and then increases up to ∼200 mV at ∼1 nm^2 at a somewhat lower rate. The inflection point observed at ∼2 nm^2 on the ΔV–A

curve may result from the fact that the fluorinated chain produces a negative ΔV, while the hydrocarbon chain produces a positive one. It is likely that the more flexible hydrocarbon spacers start lifting from the surface first and interact first upon compression, generating most of the increase in ΔV from 0 to 120 mV. For areas $<\sim 2$ nm^2, the fluorinated tails start lifting from the surface, thus compensating for the positive ΔV of the hydrocarbon spacers. Eventually, both hydrophobic parts of the molecule are lifted from the surface, while the DMP polar group remains anchored on the subphase's surface.

For areas $<\sim 0.8$ nm^2, ΔV decreases steeply to 0 mV (phase 3). It is likely that the interaction between fluorinated chains maximizes when these chains are stretched perpendicular to the substrate's surface, thus producing a strongly negative ΔV that compensates for the positive contribution of the spacers. Such a drastic change in ΔV between the beginning of phase 3 and the film collapse was not observed for fatty acid monolayers [27]. Film collapse is indicated by a sudden change of surface potential. The area and the surface pressure that are attributed to the negative maximal value of ΔV are interpreted as the area that is required by an upright molecule and as the collapse surface pressure.

The $\mu_\perp$–A curve of F8H11DMP is qualitatively similar to the ΔV–A curve and presents the same features, namely an increase of $\mu_\perp$ from 0 to 650 mD in phase 1, a decrease to $\sim$400 mD in phase 2, followed by a steep decrease down to 0 mD.

The ΔV–A and $\mu_\perp$–A isotherms of DPPC are very different from those of F8H11DMP. In the coexistence region between the gas phase and the LE phase, ΔV is almost constant ($\sim$0 mV) until a critical area ($\sim$1.1 nm^2) is reached, below which ΔV increases steeply until it reaches 300 mV. As for F8H11DMP, the changes in ΔV of DPPC occur at larger areas than the increase in surface pressure. The variation of ΔV is always positive and eventually reaches 550 mV. The LE/LC transition, clearly visible on the π–A isotherm, corresponds to a change in slope on both ΔV–A and $\mu_\perp$–A isotherms. The steep increase of both ΔV and $\mu_\perp$ that occurs at about 1 nm^2, reflecting conformational change in the monolayer state, while the surface pressure just starts increasing is due to the change of the average lateral force [28].

At high surface pressures (>30 mN m^{-1}), the fatty acyl chains are tilted with respect to the normal of the surface. The surface dipole moment shows the same trend as the ΔV–A isotherms. The value of $\mu_\perp$ changed from $\sim$50 to $\sim$560 mD via a hump at about 840 mD (Fig. 1c).

3.2. Stability of the mixed monolayers

Our general objective being to investigate the potential benefits of F8H11DMP to facilitate DPPC respreading, a 0.15 M NaCl solution was chosen as the subphase in order to mimic a biomembrane-like environment. To check the monolayers' stability, the relaxation time of the surface pressure of DPPC, F8H11DMP, and DPPC/F8H11DMP mixtures ($X_{\mathrm{F8H11DMP}} = 0.5$) was measured after compression to 35 mN m^{-1}. Figure 2 shows that the surface pressure of DPPC decreased during the first 30 min and then plateaued at $\sim$32.5 mN m^{-1}. On the other hand, no significant surface pressure variation was observed for the F8H11DMP and mixed DPPC/F8H11DMP monolayers after 1 h, reflecting their higher stability.

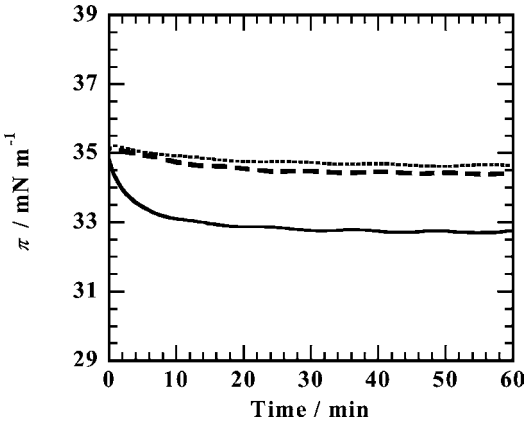

Fig. 2. Time dependence of the surface pressure (π). Langmuir monolayers were compressed up to 35 mN m^{-1} on 0.15 M NaCl at 298.2 K; the π–t measurements were then started. Solid line, DPPC; dotted line, F8H11DMP; and dashed line, DPPC/F8H11DMP (1/1).

3.3. Contributions from the CF_3 ω-group and DMP polar head group to the dipole moment

The surface potential of monolayers was often analyzed using the three-layer model proposed by Demchak and Fort [18], based on the earlier model of Davies and Rideal [29]. This model postulates independent contributions of the subphase (layer 1), polar head group (layer 2), and hydrophobic chain (layer 3). Independent dipole moments and effective local dielectric constants are attributed to each of the three layers. Other models, such as the Helmholtz model and the Vogel and Möbius model, are also available [30,31]. The differences among these models were reviewed in Ref. [32]. The conclusion was that, despite its limitations, the Demchak and Fort model provides good agreement between the $\mu_\perp$ values estimated from monolayer surface potentials and those determined from measurements made on the bulk material for various aliphatic compounds.

The estimation of $\mu_\perp$ (the vertical component of the dipole moment to the plane of the monolayer) of polar head groups and hydrocarbon chains using the Demchak and Fort model assumes condensed Langmuir monolayers with close-packed vertical chains [18,29]. Using this model in the case of the F8H11DMP LE monolayer may lead to a rough but useful estimation, which can help provide qualitative explanation of surface potential behavior.

We have thus compared the experimental values of $\mu_\perp$ in the most condensed state of the monolayer with those calcu-

lated, $\mu_{\perp\text{calc}}$, from the three-layer model-based equation,

$$\mu_{\perp\text{calc}} = (\mu_1/\varepsilon_1) + (\mu_2/\varepsilon_2) + (\mu_3/\varepsilon_3), \quad (2)$$

where μ_1/ε_1, μ_2/ε_2, and μ_3/ε_3 are the contributions of the subphase, polar head group, and hydrophobic chain, respectively.

To determine the contribution of the DMP head group, we have used a set of values introduced in Ref. [33] ($\mu_1/\varepsilon_1 = 0.025$ D, $\varepsilon_2 = 7.6$, $\varepsilon_3 = 4.2$ for CF_3), as they provide a good agreement between calculated and experimental $\mu_\perp$ values for monolayers spread on a saline phase. The same set of values has been used in a previous work in which mixtures of a zwitterionic fluorinated amphiphile derived from phosphocholine, $C_8F_{17}(CH_2)_5OP(O)O^-O(CH_2)_2N^+(CH_3)_3$ (F8C5 PC) and a fluorinated alcohol with the same hydrophobic chain, $C_8F_{17}(CH_2)_5OH$ (F8H5OH), were studied [20]. Using the value experimentally determined for F8H5OH, $\mu_\perp^{\text{F8H5OH}} = -0.44$ D, and assuming the values $\mu_1/\varepsilon_1 = 0.025$ D, $\varepsilon_2 = 7.6$, and μ_2 (OH-*gauche*) $= 1.00$ D, we were able to calculate $\mu_3/\varepsilon_3 = -0.597$ for the terminal CF_3 group, hence $\mu_3 = -2.51$ D [20].

Assuming that the value of $(\mu_3^{\text{F8H11}}/\varepsilon_3)$ for F8H11DMP is nearly equal to that of $(\mu_3^{\text{F8H5}}/\varepsilon_3)$ for F8H5OH, we obtained $\mu_2^{\text{DMP}} = 4.99$ D using

$$\mu_\perp^{\text{F8H11DMP}} = (\mu_1/\varepsilon_1) + \left(\mu_2^{\text{DMP}}/\varepsilon_2\right) + \left(\mu_3^{\text{F8H11}}/\varepsilon_3\right) = 0.085 \text{ D}. \quad (3)$$

Using the following set of parameters ($\mu_1/\varepsilon_1 = 0.025$ D, $\varepsilon_2 = 7.6$, $\mu_3 = 0.33$, and $\varepsilon_3 = 2.8$ for CH_3), we obtained the μ_2^{PC} value of 2.88 D for the phosphocholine (PC) polar head of DPPC. This value is very close to that previously reported by Taylor et al. (2.44 D) [32]. The dipole moment of DMP is 1.7 times larger than that of PC. The contribution of the DMP head group is significantly larger than that of the fluorinated chain. As a result, the surface potential of F8H11DMP never shows negative values.

3.4. Ideality of mixing

The π–A, ΔV–A, and $\mu_\perp$–A isotherms of mixed monolayers of DPPC and F8H11DMP were therefore measured for various X_{F8H11DMP} at 298.2 K on 0.15 M NaCl. For X_{F8H11DMP} lower than 0.5, π–A isotherms (Fig. 3a) display a phase transition pressure that increases almost linearly with X_{F8H11DMP} (Fig. 4). This behavior is a first evidence of the miscibility of the two components within the mixed monolayer. As it is difficult to ascertain the transition pressure values for molar fractions > 0.5 on π–A isotherms, we have investigated F8H11DMP/DPPC mixed monolayers by fluorescence microscopy (later section).

The interaction between DPPC and F8H11DMP molecules was investigated by examining whether the variation of the mean molecular areas as a function of X_{F8H11DMP} satis-

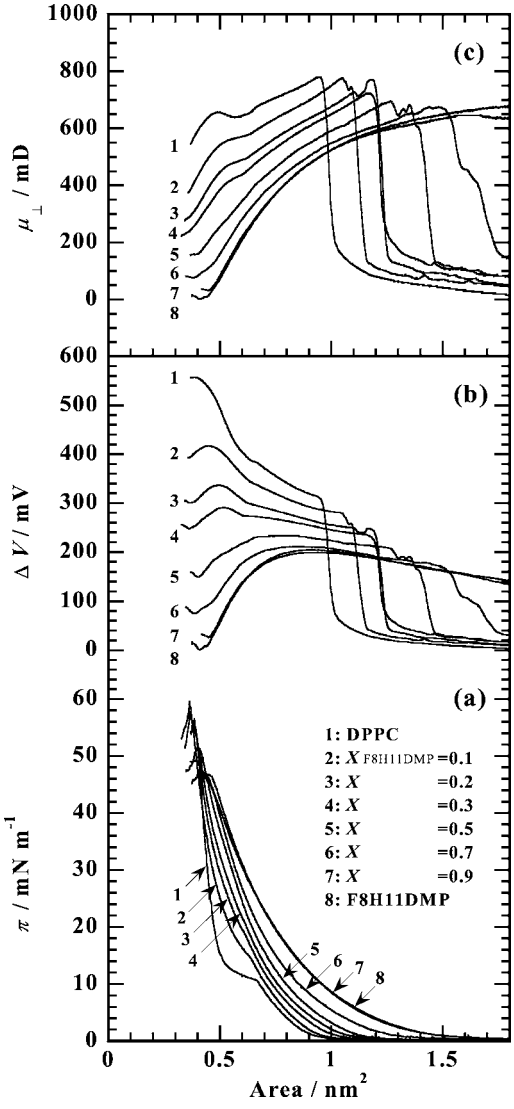

Fig. 3. (a) Surface pressure (π)–area (A) isotherms, (b) surface potential (ΔV)–A isotherms, and (c) surface dipole moment ($\mu_\perp$)–A isotherms of DPPC/F8H11DMP mixed monolayers as a function of F8H11DMP molar fraction (X_{F8H11DMP}) (on 0.15 M NaCl, 298.2 K).

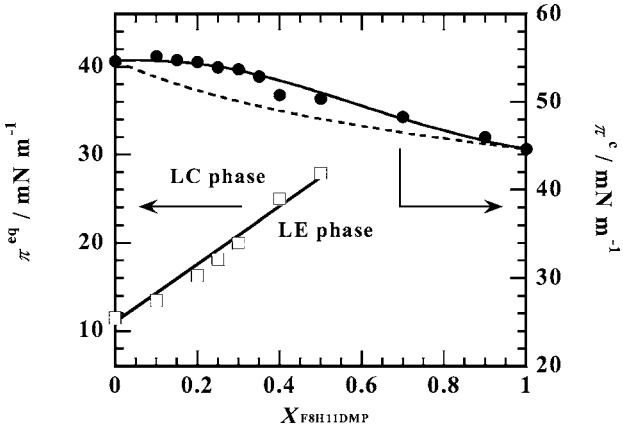

Fig. 4. Variation of the transition pressure (π^{eq}) and the collapse pressure (π^c) as a function of X_{F8H11DMP} (0.15 M NaCl, 298.2 K). The dashed line was calculated according to Eq. (4) for $\xi = 0$.

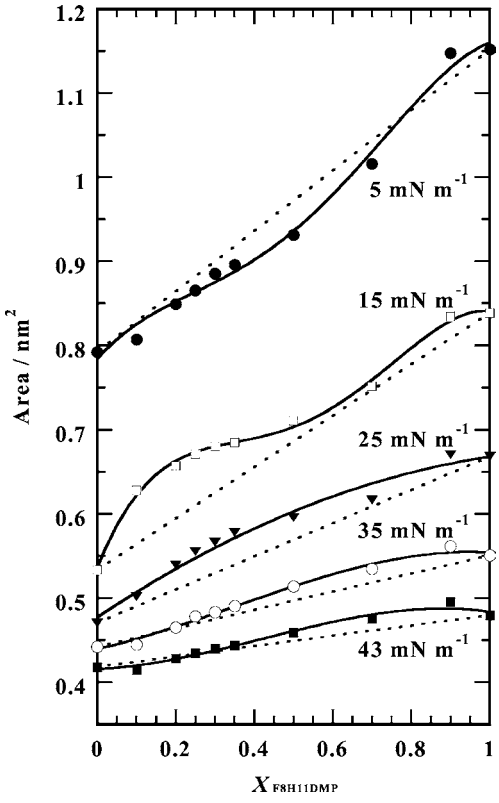

Fig. 5. Mean molecular area (A) of mixed DPPC/F8H11DMP monolayers as a function of X_{F8H11DMP} at five surface pressures. Dashed lines, theoretical variations assuming the additivity rule; markers, experimental values.

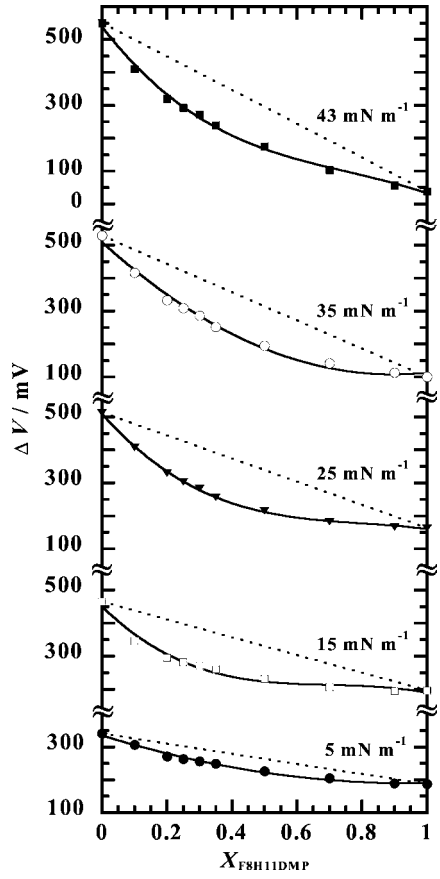

Fig. 6. Surface potential (ΔV) of mixed DPPC/F8H11DMP monolayers as a function of X_{F8H11DMP} at five surface pressures. Dashed lines, theoretical variations assuming the additivity rule; markers, experimental values.

fies the additivity rule [34]. Comparison between experimental mean molecular areas and mean molecular areas calculated for ideal mixing is shown in Fig. 5 for five surface pressures (5, 15, 25, 35, and 43 mN m^{-1}). For $\pi \leqslant 5$ mN m^{-1}, Fig. 5 shows a negative deviation from the theoretical line, indicating attractive interaction between F8H11DMP and DPPC. This may result from the fact that at such low surface pressures the interactions between DPPC and F8H11DMP (both in the LE state) are mainly governed by the attractions between polar heads. For $\pi > 5$ mN m^{-1}, positive deviations are observed, indicating repulsion between the fluorocarbon lipophobic chains of F8H11DMP and DPPC fatty acid chains. Above 35 mN m^{-1} the variation almost follows the additivity rule. This indicates that F8H11DMP and DPPC are almost ideally mixed in the monolayer. As F8H11DMP has a longer chain length than DPPC, attractive interaction between F8H11DMP hydrocarbon segments and DPPC chains are maximized and compensate for repulsions produced by the fluorocarbon segment that remains in interaction with the DPPC chain.

The influence of X_{F8H11DMP} on the ΔV–A and $\mu_{\perp}$–A isotherms is shown in Figs. 3b and 3c. Analysis of ΔV of the mixed monolayers in terms of the additivity rule is presented in Fig. 6. Comparison of the experimental data versus calculated variations clearly indicates negative deviation at all surface pressures.

3.5. Two-dimensional phase diagram

The two-dimensional phase diagram of the F8H11DMP/DPPC mixed monolayers was constructed by plotting the values of collapse pressures, π^c, as a function of X_{F8H11DMP}. A representative phase diagram at 298.2 K is shown in Fig. 4. The coexistence phase boundary between the monolayer and the bulk phases of the F8H11DMP/DPPC mixture can be simulated using the Joos equation [35],

$$1 = x_1^s \gamma_1 \exp\{(\pi_m^c - \pi_1^c)\omega_1/kT\} \exp\{\xi(x_2^s)^2\} + x_2^s \gamma_2 \exp\{(\pi_m^c - \pi_2^c)\omega_2/kT\} \exp\{\xi(x_1^s)^2\}, \quad (4)$$

where x_1^s and x_2^s denote the mole fraction at the surface of components 1 and 2, respectively, and π_1^c and π_2^c are the collapse pressures of components 1 and 2, respectively. π_m^c is the collapse pressure of the mixed monolayer at a given composition of the surface x_1^s and x_2^s, ω^1 and ω^2 are the limiting areas at the collapse points, γ_1 and γ_2 are the surface activity coefficients at the collapse points, ξ is the interaction parameter, k is the Boltzmann constant, and T the Kelvin temperature. The solid curve is made coincident with the experimental values by adjusting ξ. It is noteworthy that the DPPC/F8H11DMP monolayer produces a negative interaction parameter ($\xi = -1.3$), which implies that

the interchange energy between the two molecules is larger than the mean of the interaction energies between identical molecules. The interaction energy $\Delta\varepsilon$ was calculated to be 537 J mol^{-1}.

Thus, DPPC and F8H11DMP are miscible in the expanded state as well as in the condensed state. The interaction energy between the two components in the mixed monolayer is stronger than the mean of the interaction energies, as noted above [36–38].

3.6. Fluorescence microscopy of DPPC/F8H11DMP mixed monolayers—Flower-like patterns

In order to interpret the π–A isotherms, we investigated the monolayers by fluorescence microscopy, which provides a direct picture of the monolayers. A fluorescent dye probe was therefore incorporated into the monolayer and its distribution was determined on fluorescence micrographs. The contrast is due to differential dye solubility in LE and LC phases. Fluorescence micrographs of pure DPPC and DPPC/F8H11DMP mixed monolayers ($X_{\mathrm{F8H11DMP}} = 0.1$) spread on 0.15 M NaCl are shown in Fig. 7 for various surface pressures.

Essentially two phases of bright and dark contrast were observed, for pure DPPC (Fig. 7a), corresponding to the LE matrix and LC domains. As surface pressure increases, the proportion of dark LC phase increases at the expense of the bright LE phase. The DPPC monolayer on the 0.15 M NaCl subsolution develops LC domain structures in a qualitatively similar fashion as reported [26,39,40]. Angular, grain-like domains first appeared near the kink at $\pi^{\mathrm{eq}} \sim 11.8$ mN m^{-1}. They grew upon compression to form distorted star-shaped domains with a blurred periphery that progressively formed a network (Fig. 7a, inserted image at 20 mN m^{-1}). Above $\sim$21 mN m^{-1}, the images start loosing their crispness and the visual impression is of a progressive blurring of the domain boundaries. This blurring may be caused by the dissolution of the dye into the dye-depleted regions of the monolayer after the phase transition has been completed, i.e., when both the dye-enriched and the dye-depleted regions have become the same phase. Above 40 mN m^{-1}, it is likely that some of the probe was inserted in the dark phase areas and the intensity of the probe in the bright (fluid) domains decreased, suggesting that self-quenching has occurred because of probe molecules coming in close contact with one another.

In DPPC/F8H11DMP mixed monolayers, domains of ordered phase start forming closely after the onset of the phase transition. These domains are similar to those found in pure binary lipid monolayers [41]. For $X_{\mathrm{F8H11DMP}} = 0.1$ (Fig. 7b) domains formed at $\pi^{\mathrm{eq}} \sim 13.5$ mN m^{-1}, a value that is higher than for the pure DPPC monolayer (cf. Fig. 1). Significant differences in the fluorescence images begin to appear at $\sim$13.5 mN m^{-1}, close to the midpoint

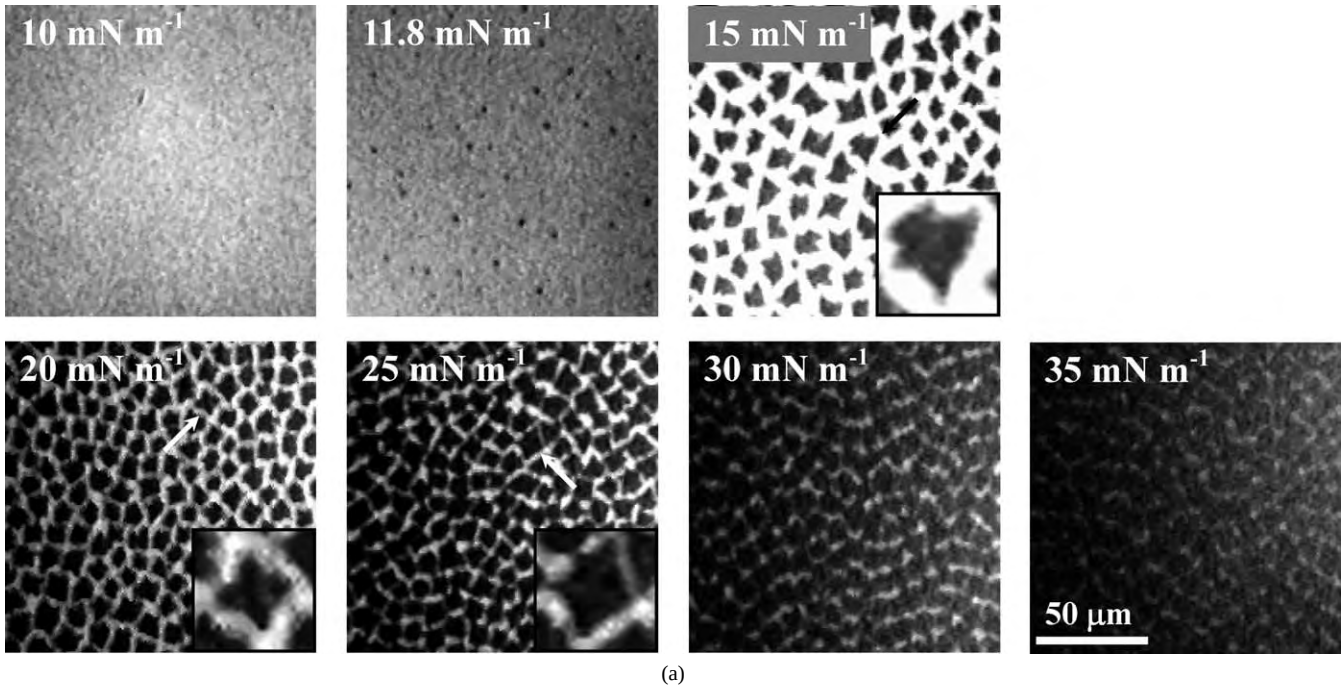

(a)

Fig. 7. Fluorescence micrographs of DPPC monolayer (a) and DPPC/F8C11DMP mixed monolayer ($X_{\mathrm{F8H11DMP}} = 0.1$) (b) observed at a compression rate of 7.3×10^{-2} nm^2 molecule^{-1} min^{-1} at 298.2 K on 0.15 M NaCl. The monolayer contained 1 mol% of fluorescent probe. The scale bar represents 50 μm. (c) Fluorescence micrographs of a DPPC/F8C11DMP mixed monolayer ($X_{\mathrm{F8H11DMP}} = 0.5$) observed at a compression rate of 7.3×10^{-2} nm^2 molecule^{-1} min^{-1} at 298.2 K on 0.15 M NaCl. The monolayer contained 1 mol% of fluorescent probe. The scale bar represents 50 μm. The mixed monolayer was in the LE fluid state at 25 mN m^{-1}, while dark LC domains were observed at 30 mN m^{-1}.

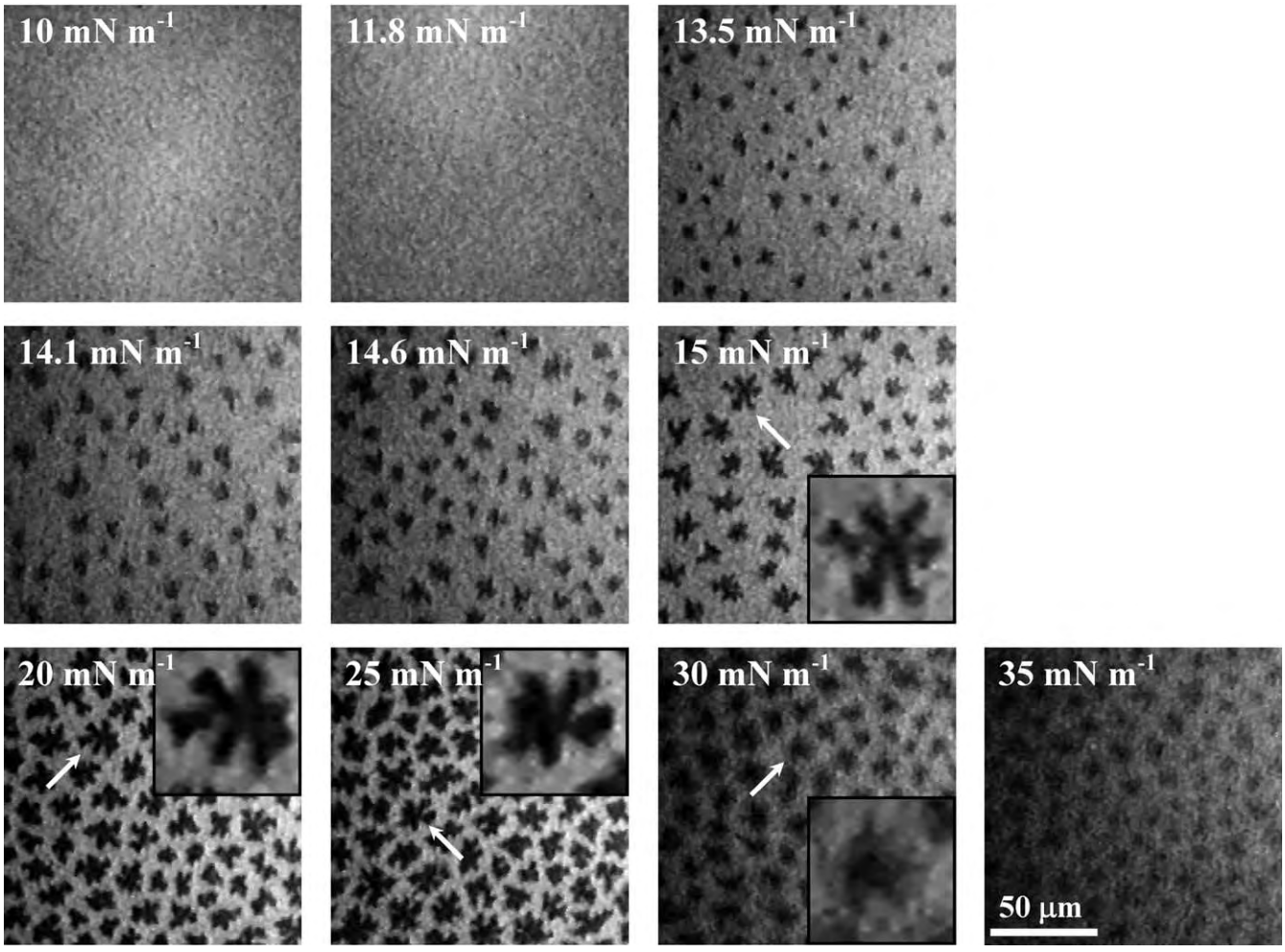

(b)

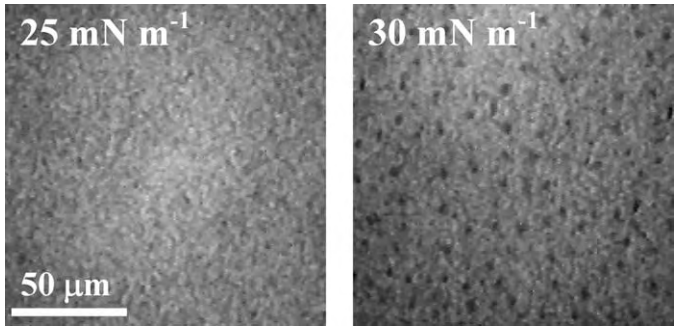

(c)

Fig. 7. (Continued.)

of the phase transition. Above 14.6 mN m^{-1}, the dark LC domains are arranged into fractal or flower-like patterns similar to those reported in Ref. [42] for DMPC (dimyristoylphosphatidylcholine)/C24:1-ceramide (*N*-[*cis*-15-tetracosenoyl]-D-sphingosine)/NBD-PC (1-palmitoyl-2-(12[(7-*nitro*-2-1,3-benzoxadizole-4-yl)amino]dodecanoyl) phosphocholine) (79/20/1, molar ratio) system. The average number of petals in the dark flower-like domains is quite constant (5.3 ± 0.4). Beginning at their periphery, solid (i.e., dye-depleted) lipid molecules are dispersed from the compact cores of the domains and are extruded into the dye-enriched phase. This leads to the formation of branches that appear at an intermediate gray level. Above 25 mN m^{-1}, the dissolved lipids form a delicate meshwork that covers the entire area between the dark flower-like pattern of the solid domains, while the ordered phase (the dark flower-

like domains) is dissolved until only micrometer-size grains remained. These grains are stable up to high lateral pressures (see images taken at 30 $mN\,m^{-1}$ in Fig. 7b). The morphologies do not visibly change in appearance up to at least 50 $mN\,m^{-1}$. One remarkable effect of the fluorinated surfactant in the DPPC/F8H11DMP mixture is thus to favor the dissolution of the ordered phase of the lipid and to induce the formation of a distinct new phase that dissolves the lipophilic dye better. This phase is therefore presumably of lower intrinsic order.

Mixed monolayers with larger F8H11DMP concentrations, i.e., up to a molar fraction of $X_{\mathrm{F8H11DMP}} = 1$ (data not shown), were also investigated. Qualitatively, similar changes in phase morphology were observed until X_{F8H11DMP} reached 0.5. However, image contrast decreased when X_{F8H11DMP} increased, so that quantitative comparison of domain morphologies was difficult to assess. In the case of $X_{\mathrm{F8H11DMP}} = 0.5$, small area fractions of dark LC domains were only observed in a narrow area interval of the π–A curve. These LC domains dissolved quickly after formation. Thereafter, the monolayer retained a fuzzy, nondescript appearance, roughly comparable to the morphology shown in Fig. 7c, however, with much less contrast. For $X_{\mathrm{F8H11DMP}} \geqslant 0.5$, no LC domains were observed; the mixed monolayers were in the LE fluid state [11].

4. Conclusions

The (perfluorooctyl)undecyldimorpholinophosphate F8H11DMP in combination with DPPC can be spread as stable monolayers on 0.15 M NaCl at 298.2 K. The π–A and ΔV–A isotherms show that the two components are miscible in the monolayer on the whole range of F8H11DMP molar fractions and surface pressures investigated. The two-dimensional phase diagram and the Joos equation allowed calculation of the interaction parameter ($\xi = -1.3$) and the energy of interaction ($\Delta\varepsilon = 537\ J\,mol^{-1}$) between DPPC and F8H11DMP. The dimorpholinophosphate polar head group strongly influences the surface potential. The Demchak and Fort model was applied to analyze the surface potential of F8H11DMP, from which the dipole moment of the polar head group was determined to be 4.99 D. Fluorescence microscopy on DPPC/F8H11DMP mixed monolayers on 0.15 M NaCl showed that F8H11DMP dissolves the ordered solid DPPC domains that form upon compression. This indicates that F8H11DMP softens the lipid, which may be crucial for the performance of this material during the dimensional changes of the monolayer imposed during inhalation–exhalation cycles.

Acknowledgments

This work was supported by grants-in-aid for the Kyushu University Foundation, which is greatly appreciated. The authors thank Monbukagakusho for a Fellowship for Junior Researcher (HC). They gratefully acknowledge Atofina (Pierre Bénite, France) for a generous gift of perfluorochemicals.

References

[1] J.G. Riess, Tetrahedron 58 (2002) 4113.
[2] M.P. Krafft, J.G. Riess, J.G. Weers, in: S. Benita (Ed.), Submicronic Emulsions in Drug Targeting and Delivery, Harwood Academic, Amsterdam, 1998, p. 235.
[3] J.G. Riess, Chem. Rev. 101 (2001) 2797.
[4] E.G. Schutt, D.H. Klein, R.M. Mattrey, J.G. Riess, Angew. Chem. Int. Ed. Engl. (2002), in press.
[5] M.P. Krafft, Adv. Drug Deliv. Rev. 47 (2001) 209.
[6] V.M. Sadtler, M.P. Krafft, J.G. Riess, Angew. Chem. Int. Ed. Engl. 35 (1996) 1976.
[7] H.M. Courrier, T.F. Vandamme, M.P. Krafft (2002), in preparation.
[8] N. Butz, C. Porté, H.M. Courrier, M.P. Krafft, T.F. Vandamme, Int. J. Pharm. 238 (2002) 257.
[9] H.M. Courrier, M.P. Krafft, C. Porté, N. Butz, F. Pons, N. Frossard, A. Rémy-Kristensen, Y. Mély, T.F. Vandamme, Biomaterials (2003), in press.
[10] J.-B. Brubach, A. Mermet, A. Filabozzi, A. Gerschel, D. Lairez, M.P. Krafft, P. Roy, J. Phys. Chem. B 105 (2001) 430.
[11] H.M. Courrier, T.F. Vandamme, M.P. Krafft, S. Nakamura, O. Shibata, Colloids Surf. A 215 (2003) 33.
[12] T. Imae, T. Takeshita, M. Kato, Langmuir 16 (2000) 612.
[13] H. Lehmler, P. Bummer, J. Colloid Interface Sci. 249 (2002) 381.
[14] H. Matuo, K. Motomura, R. Matuura, Chem. Phys. Lipids 28 (1981) 281.
[15] S. Yamamoto, O. Shibata, S. Lee, G. Sugihara, Prog. Anesthesiol. Mech. 3 (1995) 25.
[16] O. Shibata, S. Yamamoto, S. Lee, G. Sugihara, J. Colloid Interface Sci. 184 (1996) 201.
[17] H. Lehmler, M. Jay, P. Bummer, Langmuir 16 (2000) 10161.
[18] R.J. Demchak, T. Fort Jr., J. Colloid Interface Sci. 46 (1974) 191.
[19] V.M. Sadtler, F. Jeanneaux, M.P. Krafft, J. Rabai, J.G. Riess, New J. Chem. 22 (1998) 609.
[20] O. Shibata, M. Krafft, Langmuir 16 (2000) 10281.
[21] O. Shibata, Y. Moroi, M. Saito, R. Matuura, Langmuir 8 (1992) 1806.
[22] O. Shibata, H. Miyoshi, S. Nagadome, G. Sugihara, H.J. Igimi, J. Colloid Interface Sci. 146 (1991) 595.
[23] O. Shibata, Y. Moroi, M. Saito, R. Matuura, Thin Solid Films 123 (1998) 327.
[24] T. Kato, M. Kameyama, M. Ehara, K.-I. Iimura, Langmuir 14 (1998) 1786.
[25] O. Albrecht, H. Gruler, E. Sacknann, J. Phys. (France) 39 (1978) 301.
[26] M. Lösche, E. Sackmann, H. Möhwald, Ber. Bunsen-Ges. Phys. Chem. 87 (1983) 848.
[27] O. Shibata, Y. Moroi, M. Saito, R. Matuura, Thin Solid Films 242 (1994) 273.
[28] H.J. Morgan, D.M. Taylor, O.N.J. Oliveira, Biochim. Biophys. Acta 1062 (1991) 149.
[29] J.T. Davies, E.K. Rideal, Interfacial Phenomena, 2nd ed., Academic Press, New York, 1963.
[30] V. Vogel, D. Möbius, J. Colloid Interface Sci. 126 (1988) 408.
[31] V. Vogel, D. Möbius, Thin Solid Films 159 (1988) 73.
[32] D.M. Taylor, O.N.J. Oliveira, H.J. Morgan, J. Colloid Interface Sci. 139 (1990) 508.
[33] J.G. Petrov, E.E. Polymeropoulos, H.J. Möhwald, Phys. Chem. 100 (1996) 9860.
[34] J. Marsden, J.H. Schulman, Trans. Faraday Soc. 34 (1938) 748; D.O. Shah, J.H. Schulman, J. Lipid Res. 8 (1967) 215.

[35] P. Joos, R.A. Demel, Biochim. Biophys. Acta 183 (1969) 447.
[36] H. Matuo, N. Yoshida, K. Motomura, R. Matuura, Bull. Chem. Soc. Jpn. 52 (1979) 667.
[37] H. Matuo, K. Motomura, R. Matuura, Bull. Chem. Soc. Jpn. 54 (1981) 2205.
[38] H. Matuo, D.K. Rice, D.M. Balthasar, D.A. Cadenhead, Chem. Phys. Lipids 30 (1982) 367.
[39] M. Lösche, H.-P. Duwe, H.J. Möhwald, J. Colloid Interface Sci. 126 (1988) 432.
[40] K. Nag, K.M.W. Keough, Biophys. J. 65 (1993) 1019.
[41] P. Krüger, M. Schalke, Z. Wang, R.H. Notter, R.A. Dluhy, M. Lösche, Biophys. J. 77 (1999) 903.
[42] J.M. Holopainen, L.B. Howard, E.B. Rhoderick, P.K.J. Kinnumen, Biophys. J. 80 (2001) 765.